



SDSS J134441.83+204408.3: A Highly Asynchronous Short-period Magnetic Cataclysmic Variable with a 56 MG Field Strength

Colin Littlefield¹ , Paul A. Mason^{2,3} , Peter Garnavich⁴ , Paula Szkody⁵ , John Thorstensen⁶ , Simone Scaringi⁷ ,
Krystian Iłkiewicz^{7,8} , Mark R. Kennedy⁹ , and Natalie Wells^{2,3}

¹ Bay Area Environmental Research Institute, Moffett Field, CA 94035, USA

² New Mexico State University, MSC 3DA, Las Cruces, NM 88003, USA

³ Picture Rocks Observatory, 1025 S. Solano Dr. Suite D., Las Cruces, NM 88001, USA

⁴ Department of Physics and Astronomy, University of Notre Dame, Notre Dame, IN 46556, USA

⁵ Department of Astronomy, University of Washington, Seattle, WA 98195, USA

⁶ Department of Physics and Astronomy, 6127 Wilder Laboratory, Dartmouth College, Hanover, NH 03755-3528, USA

⁷ Centre for Extragalactic Astronomy, Department of Physics, Durham University, South Road, Durham DH1 3LE, UK

⁸ Astronomical Observatory, University of Warsaw, Al. Ujazdowskie 4, 00-478 Warszawa, Poland

⁹ Department of Physics, University College Cork, Cork, Ireland

Received 2022 December 9; accepted 2022 December 22; published 2023 February 1

Abstract

When the accreting white dwarf in a magnetic cataclysmic variable star (mCV) has a field strength in excess of 10 MG, it is expected to synchronize its rotational frequency to the binary orbit frequency, particularly at small binary separations, due to the steep radial dependence of the magnetic field. We report the discovery of an mCV (SDSS J134441.83+204408.3, hereafter J1344) that defies this expectation by displaying asynchronous rotation ($P_{\text{spin}}/P_{\text{orb}} = 0.893$) in spite of a high surface field strength ($B = 56$ MG) and a short orbital period (114 minutes). Previously misidentified as a synchronously rotating mCV, J1344 was observed by Transiting Exoplanet Survey Satellite during sector 50, and the resulting power spectrum shows distinct spin and orbital frequencies, along with various sidebands and harmonics. Although there are several other asynchronous mCVs at short orbital periods, the presence of cyclotron humps in J1344's Sloan Digital Sky Survey spectrum makes it possible to directly measure the field strength in the cyclotron-emitting region, and while a previously study estimated 65 MG based on its identification of two cyclotron humps, we revise this to 56 ± 2 MG based on the detection of a third hump and on our modeling of the cyclotron spectrum. Short-period mCVs with field strengths above 10 MG are normally expected to be synchronous, so the highly asynchronous rotation in J1344 presents an interesting challenge for theoretical studies of spin-period evolution.

Unified Astronomy Thesaurus concepts: Cataclysmic variable stars (203); DQ Herculis stars (407); AM Herculis stars (32); Stellar magnetic fields (1610)

1. Introduction

1.1. Asynchronous Magnetic Cataclysmic Variables

One of the most-studied aspects of magnetic cataclysmic variable stars (mCVs) is the evolution of the spin period of the primary star, an accreting, magnetized white dwarf (WD). WDs with field strengths above $B \sim 10$ MG are expected to rotate synchronously with the binary orbit, such that $P_{\text{spin}} = P_{\text{orb}}$. These systems are known as polars. At lower field strengths, the WD rotates significantly faster than the binary orbit; these systems are known as intermediate polars (IPs).

Somewhat paradoxically, a small number of polars are desynchronized by $\lesssim 3\%$. However, these asynchronous polars (APs) are widely thought to be formerly synchronous rotators that are returning to synchronous rotation. A recent nova eruption is the most commonly invoked mechanism for breaking the synchronous rotation. The asynchronous rotation in APs is a temporary disequilibrium, which distinguishes them from IPs, for which there are several proposed equilibrium conditions in which $P_{\text{spin}} < P_{\text{orb}}$.

Although APs once had very distinct $P_{\text{spin}}/P_{\text{orb}}$ ratios compared to IPs, the unusual systems Paloma ($P_{\text{spin}}/P_{\text{orb}} = 0.87$; Schwarz et al. 2007; Joshi et al. 2016; Littlefield et al. 2022) and Swift J0503.7-2819 ($P_{\text{spin}}/P_{\text{orb}} = 0.8$; Halpern 2022; Rawat et al. 2022) have blurred the once-clear line of division between the APs and IPs.¹⁰ Throughout this paper, we use the neutral term “asynchronous mCV” to refer to systems in which it is unknown whether the observed asynchronous rotation is an equilibrium condition.¹¹

Long, uninterrupted light curves of asynchronous mCVs are of great value because they provide coverage of the beat period between the spin and orbital periods. The beat period is the time required for the WD to complete a single rotation within the binary rest frame, and the differential rotation modulates the geometry of the accretion flow. Because this period can be days, weeks, or even months long, it is often infeasible to observe from the ground. The Kepler spacecraft and the

¹⁰ Halpern (2022) identifies two possible sets of frequency identifications, resulting in either $P_{\text{spin}}/P_{\text{orb}} = 0.80$ or $P_{\text{spin}}/P_{\text{orb}} = 0.89$. We agree with Rawat et al. (2022) that the available data favor $P_{\text{spin}}/P_{\text{orb}} = 0.8$ for Swift J0503.7-2819, but in light of the complexities discussed by Halpern (2022), $P_{\text{spin}}/P_{\text{orb}}$ still requires observational confirmation.

¹¹ The existing terminology for Paloma-type systems is inelegant, as they are often referred to as either “nearly synchronous IPs” or “highly asynchronous polars.”



Transiting Exoplanet Survey Satellite (TESS) have observed several APs, resulting in a flurry of publications about the APs: CD Ind (Hakala et al. 2019; Littlefield et al. 2019; Mason et al. 2020), V1500 Cyg (Wang et al. 2021), BY Cam (Mason et al. 2022), and SDSS J0846 (Littlefield et al. 2023), as well as Paloma (Littlefield et al. 2023) and Swift J0503.7-2819 (Halpern 2022; Rawat et al. 2022).

1.2. SDSS J134441.83+204408.3

The subject of this study, SDSS J134441.83+204408.3 (hereafter J1344), presents a challenge to these classifications. J1344 has been included in several photometric and spectroscopic studies, but it has not received in-depth attention. Szkody et al. (2011) reported its Sloan Digital Sky Survey (SDSS) spectrum and classified it as a likely polar, based on a conspicuous cyclotron hump, the presence of H α and H β emission, and a large ($\sim 400 \text{ km s}^{-1}$) radial-velocity amplitude. Follow-up time-series photometry by Szkody et al. (2014) found that the light curve changed dramatically over the course of days. The same study also reanalyzed the SDSS spectrum and proposed a candidate field strength of 65 MG. Most recently, Thorstensen et al. (2020) reported additional spectroscopy and photometry, identifying a likely orbital period of 102 minutes. The Thorstensen et al. (2020) spectrum showed He I and He II emission, neither of which was visible in the SDSS spectrum.

Bailer-Jones et al. (2021) estimate J1344’s distance to be 599_{-46}^{+53} pc using geometric priors and the Gaia eDR3 parallax (Gaia Collaboration et al. 2016, 2021).

2. Data

The TESS observed J1344 from 2022 March 26 until 2022 April 22 at a 2 minute cadence.¹² The TESS pipeline produced two light curves of J1344: one that presents the simple aperture photometry (SAP) of J1344 and another that shows the preconditioned SAP (PDCSAP) flux. Both are based on the same underlying observations, except that PDCSAP flux attempts to correct the SAP light curve for systematic artifacts. We saw no significant differences in the two light curves and elected to use the SAP data for our analysis. We specified a “hard” quality bitmask to exclude sections of the light curve of suspect quality, resulting in several large gaps in the light curve (Figure 1).

To establish the historical context for J1344’s accretion rate during the TESS observations, we downloaded the ATLAS light curve. The ATLAS data (Figure 1) show that J1344 was near magnitude 19 in both the *c*- and *o*-bands during the TESS observation. For context, J1344 was approximately 1 mag brighter in 2016 February–March, when Thorstensen et al. (2020) obtained the time-series spectroscopy. Thus, the Thorstensen et al. (2020) spectra were obtained when the accretion rate was higher.

Our data set also includes four previously unpublished light curves of J1344 from 2018 June 12, 13, 14, and 15. These data were obtained with the Otto Struve (2.1 m) telescope of the McDonald Observatory at a cadence of 5 s, without dead time. A broadband optical filter covering the Johnson BVR range was used and the images were dark-subtracted and flat-field-corrected

using routines in Python. The nightly light curves are shown in Figure 2.

3. Analysis

3.1. TESS Photometry

Unfortunately, the signal-to-noise ratio of the TESS light curve is too low to permit an in-depth study of its temporal evolution, but the power spectrum of the full data set (Figure 1) contains a series of high-frequency sidebands and harmonics, similar to the TESS and K2 power spectra of other asynchronous polars. If J1344 were synchronous, we would observe only the orbital frequency Ω and its harmonics, so the presence of the sideband frequencies unequivocally establishes that $\omega \neq \Omega$.

While it is relatively easy to establish the presence of asynchronous rotation, ascertaining the identities of the various signals is a more fraught process. The largest-amplitude signal is at $14.166 \text{ cycles day}^{-1}$, and it is identical to the Thorstensen et al. (2020) spectroscopic period of $P_{\text{spec}} = 0.070592(4) \text{ day}$ (102 minutes), measured from the radial-velocity variations of the H α emission. Thorstensen et al. (2020) interpreted this as the orbital period of the binary, which would be the proper interpretation in a synchronous polar (as J1344 was believed to be at the time). However, in an asynchronous system, it is possible that some (or even most) of the emitting material is trapped in the WD’s magnetosphere, which would cause its radial-velocity variations to be modulated at ω rather than Ω . Encountering this very problem in a study of the asynchronous mCV Swift J0503.7-2819, Halpern (2022) argued that a spectroscopic period based on the entire line will most likely yield the orbital period rather than the spin period. However, he also pointed out that this interpretation is circumstantial.

We think that the spectroscopic frequency in J1344 corresponds to the WD spin. The main justification for this inference is the high surface field strength of the WD ($B = 56 \pm 2 \text{ MG}$; see Section 3.3) and the rather modest accretion rate during the Thorstensen et al. (2020) spectroscopic observations (as evidenced by the modest strength of He II $\lambda 4686 \text{ \AA}$ in his spectra). A high field strength, combined with a moderately low mass-transfer rate, will reduce the extent of the ballistic region of the accretion flow (which rotates at Ω) and increase the size of the magnetically confined flow (which rotates at ω).

We also considered the possibility that the signal at $14.166 \text{ cycles day}^{-1}$ is the $2\omega - \Omega$ sideband, as Littlefield et al. (2019) and Mason et al. (2020) argued for CD Ind. However this identification in J1344 appears unlikely for two reasons. First, it would require that the orbital frequency and its harmonics have almost no power in the TESS power spectrum, even though ω would not be similarly impacted. Second, following the approach of Mason et al. (2020), we checked whether the dominant short- and long-term periodicities in the light curve agree. We did this by computing power spectra in 0.2 day segments, summing them, and comparing the resulting power spectrum against that of the full data set. The rationale of this exercise, as explained by Mason et al. (2020), is that pole switching redistributes power from its intrinsic frequency (ω) into sidebands (particularly $2\omega - \Omega$); if the light curve is divided into short segments that contain no pole switching, their power spectrum should show the true spin frequency. We find that with J1344, the short- and long-term periodicities agree, which suggests that the power spectrum in Figure 1 has not been contaminated.

¹² The TESS 2 minute cadence light curves are available on MAST: doi:10.17909/19-nmc8-f686.

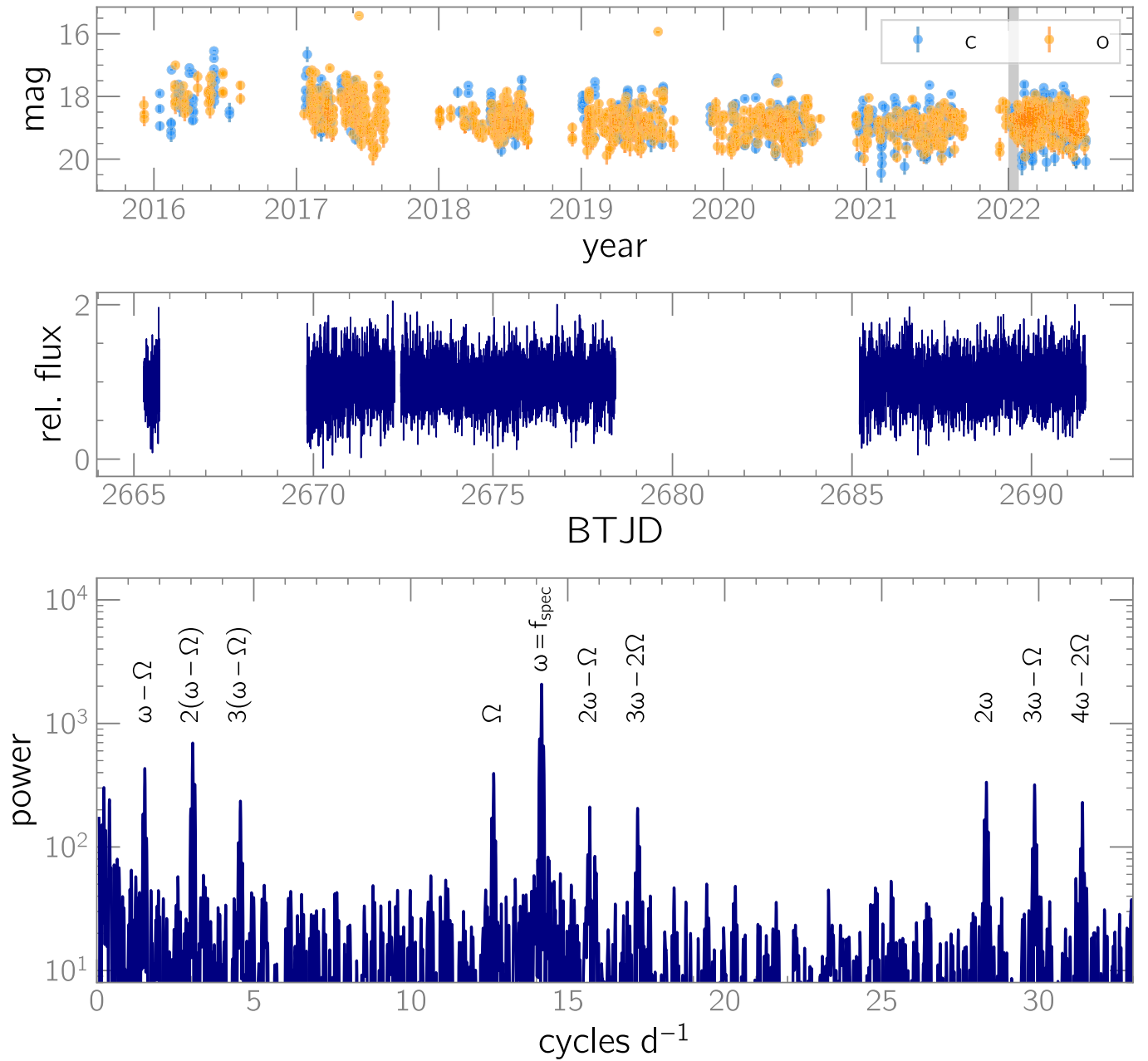


Figure 1. Top: long-term ATLAS light curve of J1344, consisting of *c*- and *o*-band observations. The shaded region indicates the time of the TESS observations. Middle: TESS light curve of J1344. Bottom: power spectrum of the TESS light curve. As we discuss in the text, we interpret the Thorstensen et al. (2020) spectroscopic frequency as the spin frequency ω , but it is conceivable that it is actually the orbital frequency Ω . However, the identification of the beat frequency $\omega - \Omega$ and its harmonics is secure, and the very presence of this frequency establishes that J1344 is an asynchronous rotator.

The beat frequency ($\omega - \Omega = 1.52 \text{ cycles day}^{-1}$) is directly observable in the TESS power spectrum, and since it is defined as the difference between the spin and orbital frequencies, our tentative identification of ω enables us to identify the likely orbital frequency as $\Omega = 12.641 \text{ cycles day}^{-1}$ by simply subtracting $\omega - \Omega$ from ω . The resulting $P_{\text{spin}}/P_{\text{orb}}$ is 0.893. If the Thorstensen et al. (2020) spectroscopic period is instead identical to Ω , $P_{\text{spin}}/P_{\text{orb}} = 0.903$. Thus, even if we have confused ω and Ω , the net result would be that J1344 is only slightly closer to being synchronous.

3.2. Ground-based Photometry

The asynchronous rotation revealed by TESS can be easily reconciled with previous photometric observations and with the

four light curves presented in Figure 2. Together, Figure 4 in Szkody et al. (2014) and Figure 18 in Thorstensen et al. (2020) show seven light curves of J1344 from different nights, and their morphology varies profoundly. The same is true of our ground-based photometry (Figure 2). This behavior is common for asynchronous polars (e.g., Mason et al. 1989; Hakala et al. 2019; Littlefield et al. 2019) because the accretion flow couples to different field lines throughout the beat cycle in response to the asynchronous rotation. Our identification of J1344 as an asynchronous mCV therefore offers a simple interpretation of the seemingly erratic behavior noted by previous studies. Indeed, in Figure 2, the profile of the light curve can be seen returning to its original shape after the passage of an integer number of beat cycles.

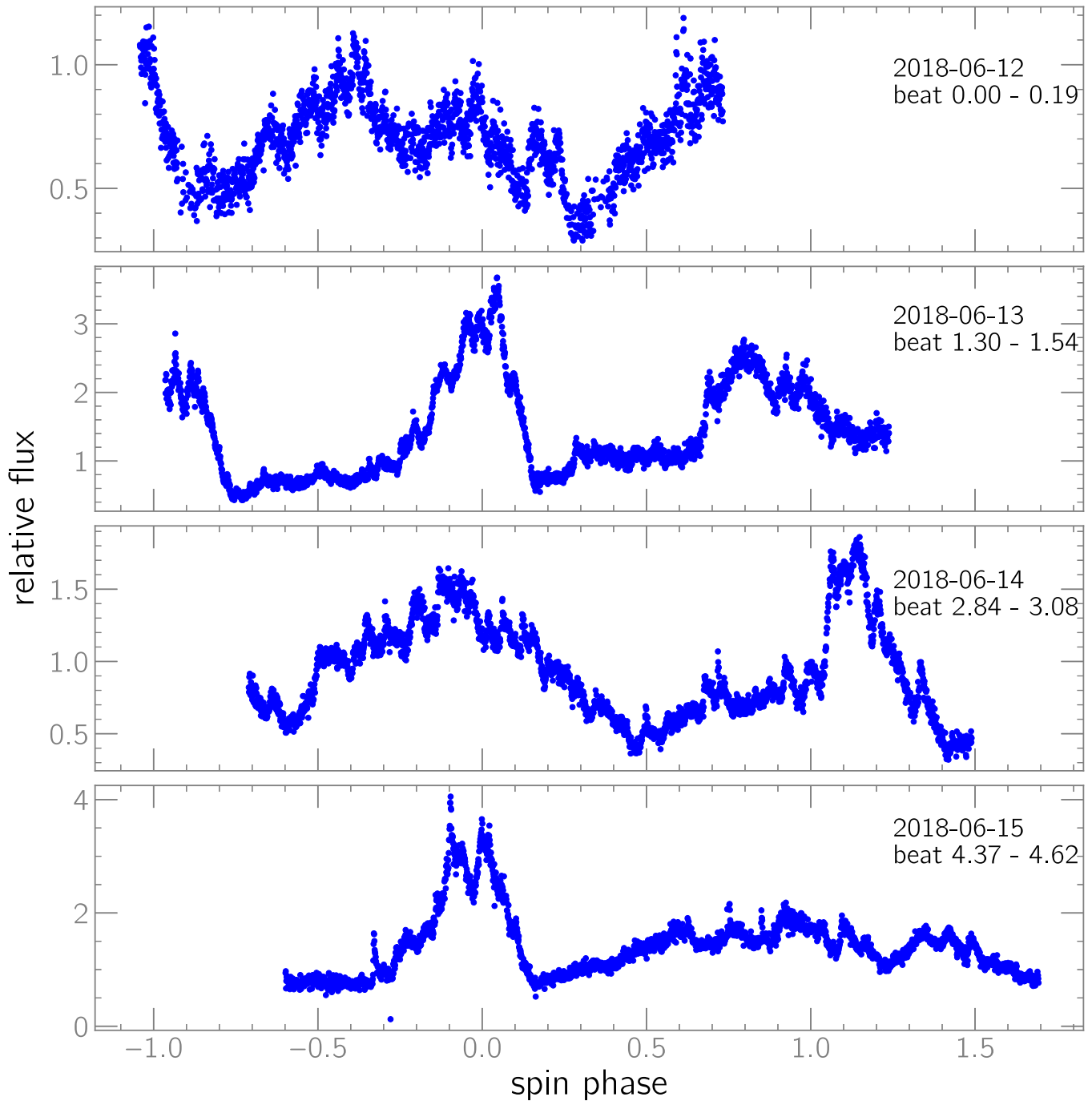


Figure 2. High-speed photometry of J1344 obtained on four consecutive nights in 2018 June. Each panel indicates the UT date at the start of the light curve and the beat cycles covered by each light curve. Spin phase 0.0 was arbitrarily chosen to correspond with the strongest peak in the light curve from 2018 June 13, while beat phase 0.0 corresponds with the first point in the June 12 light curve.

In addition, the ground-based light curves confirm that the variability observed in the TESS light curve is attributable to J1344 as opposed to a blended background source.

3.3. Magnetic Field Strength

The SDSS spectrum from Szkody et al. (2011) is of great value because it captured J1344 in a low-accretion state. Only five emission lines ($H\alpha$, $H\beta$, $H\gamma$, $H\delta$, and $\text{He I } \lambda 5876 \text{ \AA}$) are detectable in that spectrum, and the weakness of these lines, combined with the complete absence of He II emission, suggests that there was no accretion shock at the time of the

SDSS observation. This is possible only at extremely low accretion rates, though the presence of an obvious cyclotron hump near 520 nm confirms that there was very modest accretion onto the WD when the SDSS spectrum was obtained. In contrast, the time-series spectroscopy presented in Thorstensen et al. (2020), which was obtained during a state of increased accretion compared to the SDSS spectrum, shows significant He II emission, and only the 520 nm hump is discernible.

The field strength of the cyclotron-emitting region can be estimated from the wavelengths at which cyclotron humps

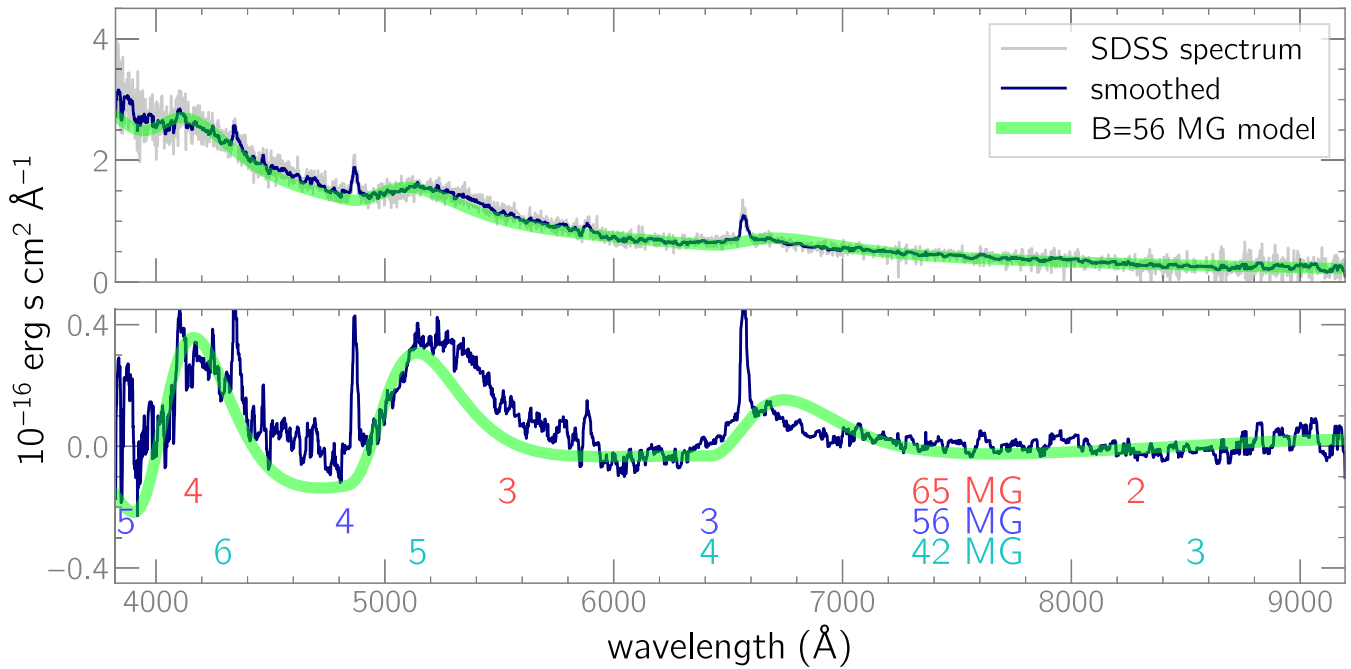


Figure 3. Top: SDSS spectrum of J1344, with the best-fit cyclotron model spectrum. Bottom: median-smoothed spectrum from the top panel after subtraction of the continuum. Cyclotron harmonics near 4100, 5200, and 6600 Å are visible. The expected positions of the n th cyclotron harmonics are labeled for three different field strengths: the original estimate of 65 MG (shown in red) from Szkody et al. (2011), 56 MG (blue), and 42 MG (cyan). The 65 MG field cannot account for the hump near 650 nm, while a 42 MG field would produce a hump near 860 nm. The 56 MG model (green line), in contrast, successfully predicts the three humps that are visible.

appear. Szkody et al. (2011) identified two humps in the SDSS spectrum consistent with the third and fourth cyclotron harmonics produced in a 65 MG field. However, they pointed out that the $n=2$ harmonic near 8200 Å was absent in the SDSS spectrum, even though the SDSS spectrum provides adequate wavelength coverage. Our reexamination of the SDSS spectrum favors a somewhat lower field strength. Figure 3 shows the presence of at least three cyclotron humps in the SDSS spectrum near 4200, 5200, and 6600 Å. We find that these three humps can be explained as harmonics 3–5 in a $B \sim 56$ MG field or as harmonics 4–6 at $B \sim 42$ MG.

To distinguish between these two possibilities, we fit the SDSS spectrum with a homogeneous cyclotron-spectrum model (Chanmugam & Wagner 1979), a technique that is more precise than simply computing the approximate wavelengths of cyclotron humps. A cyclotron spectrum was calculated for magnetic fields between 40 and 70 MG, with the wavelengths of the harmonics best matching the humps in the observed spectrum near 56 MG. A value of 55 MG better matches the $n=4$ harmonic peak while 57 MG improves the fit to the $n=3$ harmonic peak. Therefore, we estimate the uncertainty on the field to be ± 2 MG. The cyclotron spectrum was added to a continuum function varying as $\lambda^{-\alpha}$, and the electron temperature T was varied to approximate the width of the cyclotron humps. A temperature of $kT \approx 12 \pm 3$ keV was found to provide a fair match to the widths. The best-fit cyclotron spectrum, shown in Figure 3, has a field strength of $B = 56 \pm 2$ MG, and we adopt this as the surface field strength of the WD.

Does the photosphere of the WD contribute significantly to the observed SDSS spectrum? To investigate this possibility, we scaled the Koester (2010) spectral templates for nonmagnetic WDs, varying both the effective temperature and surface gravity, to the Gaia distance of J1344 (599 pc). The three-

dimensional extinction maps of Green et al. (2019) indicate negligible reddening along the line of sight to J1344, so there is no need to deredden the SDSS spectrum, which we find to be significantly brighter than expected for a WD at that distance (Figure 4).¹³ The scaled spectral templates can reach the SDSS continuum only for implausibly low WD masses or WD temperatures that are so high they contradict the Gaia near-ultraviolet (NUV)/far-ultraviolet (FUV) measurements. We conclude that the blue continuum of the SDSS spectrum cannot be attributed exclusively to the WD photosphere, which suggests that cyclotron radiation is the most likely culprit for the undulations in the SDSS spectrum, consistent with the interpretation of Szkody et al. (2011).

4. Discussion

4.1. Comparing J1344 to Other mCVs

What makes J1344 remarkable is the combination of three parameters: its moderately high magnetic-field strength, its short orbital period, and its high degree of asynchronism. Together, these properties paint an interesting picture of an mCV that would normally be expected to be synchronous, but is not.

J1344 spin-to-orbit ratio of $P_{\text{spin}}/P_{\text{orb}} = 0.893$ is most unusual for an mCV. In IPs, $P_{\text{spin}}/P_{\text{orb}} \lesssim 0.1$ is very common, and only a handful of short-orbital-period IPs show $P_{\text{spin}}/P_{\text{orb}} \gg 0.1$ (Figure 5). EX Hya has long been the benchmark system in this regard, and its unusual $P_{\text{spin}}/P_{\text{orb}}$ of 0.68 has received significant theoretical attention (e.g., King & Wynn 1999). While EX Hya is famous for being a slowly

¹³ We neglect the spectroscopic contribution of the (presumed) mid-to-late M companion star, as it is not a plausible origin of the blue continuum and is absent even at the red end of the SDSS spectrum.

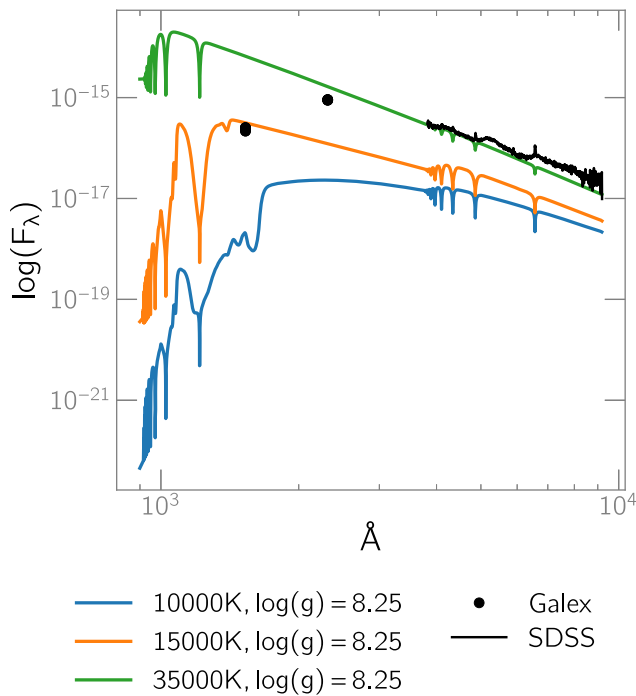


Figure 4. Spectral energy distribution of J1344 compared to selected Koester (2010) WD spectral templates for $M \sim 0.8 M_{\odot}$, scaled to the Gaia eDR3 distance of J1344. The SED therefore cannot be explained solely by the WD’s photospheric contribution; while a hot WD could explain the optical continuum, it significantly overestimates the Galex NUV/FUV measurements. Furthermore, while the SED does not pinpoint a unique WD effective temperature, it suggests that the WD is not particularly hot, providing evidence against a recent nova.

rotating IP in a hypothesized unique spin equilibrium (King & Wynn 1999; Norton et al. 2004), Paloma ($P_{\text{spin}}/P_{\text{orb}} = 0.87$; Schwarz et al. 2007; Joshi et al. 2016; Littlefield et al. 2023) has been known for nearly two decades as a solitary outlier that blurs the dividing line between IPs and APs. But with the recent identifications of J1344 and Swift J0503.7-2819 (Halpern 2022; Rawat et al. 2022), it is becoming clear that Paloma’s $P_{\text{spin}}/P_{\text{orb}}$ is not as extreme as it might have once appeared (Figure 5).

Likewise, the magnetic-field strength in J1344 is notably high in comparison to the relatively few asynchronous mCVs for which an estimated field strength has been published.¹⁴ The detection of polarized emission in spectropolarimetry has led to estimates of $\sim 9\text{--}27$ MG (Vaeth 1997) and $B = 31.5 \pm 0.8$ MG in V2400 Oph and V405 Aur (Pirola et al. 2008), respectively. As for the APs, our review turns up four systems with reliable magnetic-field estimates: 11 ± 2 MG in CD Ind (Schwope et al. 1997), 40.8 MG in BY Cam (Cropper et al. 1989), $B \lesssim 20$ MG in IGR J19552+0044 (Tovmassian et al. 2017), and $B_1 = 72$ MG, $B_2 = 105$ MG for two separate accretion regions in the old nova V1500 Cyg (Harrison & Campbell 2018). Indeed, J1344’s field strength is more typical of synchronous polars (Ferrario et al. 2015). Unfortunately, the magnetic-field strength has not been measured in either Paloma or Swift J0503.7-2819, the two mCVs that have the most similar values of $P_{\text{spin}}/P_{\text{orb}}$ to that of J1344.

The third distinguishing property of J1344 is that it has a short orbital period and therefore a relatively small binary

¹⁴ We do not consider the detached system AR Sco because its field strength has not been conclusively established.

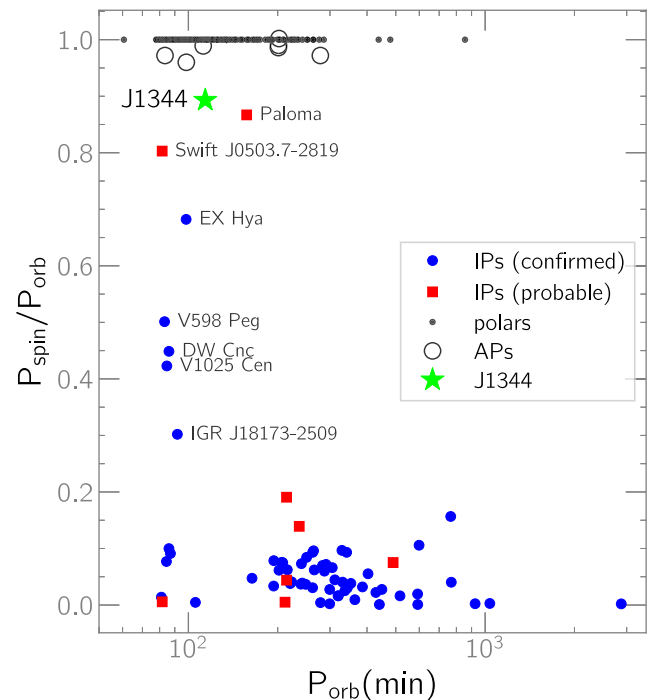


Figure 5. $P_{\text{spin}}/P_{\text{orb}}$ as a function of orbital period in mCVs. The IP data were downloaded from Koji Mukai’s IP catalog; blue markers represent the IPs assessed by Mukai to be either “confirmed” and “ironclad,” while red markers are “probable” IPs. We use Mukai’s compilation of spin periods, except for Swift J0503.7-2819 and Paloma, whose spin periods are from Rawat et al. (2022) and Littlefield et al. (2023), respectively. The AP data are from Table 1 in Littlefield et al. (2023), and the periods of the polars are from the AAVSO International Variable Star Index catalog. We have labeled J1344 as well as individual mCVs with $0.25 \leq P_{\text{spin}}/P_{\text{orb}} \leq 0.9$.

separation. As the binary orbit shrinks, the secondary will interact more strongly with the WD’s magnetosphere, which greatly facilitates synchronization (Chanmugam & Ray 1984); moreover, the secular mass-transfer rate below the period gap is significantly lower than that above the gap (e.g., Knigge et al. 2011), which reduces the spin-up torque caused by accretion. As we discuss in the following subsection, these properties tend to favor synchronization.

4.2. The Nature of Asynchronous Rotation in J1344

As noted earlier, a short orbital period increases the synchronization torque while decreasing the opposing accretion torque, and this principle has led to speculation that IPs can evolve into polars when they cross the period gap (Chanmugam & Ray 1984). Although Figure 5 might seem to lend credence to this theory by showing that high- $P_{\text{spin}}/P_{\text{orb}}$ mCVs occur exclusively at short orbital periods, this appearance is misleading, as (1) there is a predicted continuum of rotational equilibria for EX Hya-like systems (King & Wynn 1999; Norton et al. 2004) and (2) the synchronization timescales in Chanmugam & Ray (1984) and Schreiber et al. (2021) are several Myr, which is very short compared to the multi-Gyr lifetime of a CV. The probability of detecting a system synchronizing for the first time is therefore rather low.

An important step toward understanding the asynchronous rotation in J1344 is knowing whether the WD is in rotational equilibrium or is instead evolving toward synchronous rotation. Without knowledge of the long-term behavior of J1344’s spin-period derivative, we must remain agnostic as to whether the

system is in rotational equilibrium, which occurs when the spin-up torque of accretion is balanced by the countervailing drag of the magnetic field through the accretion flow and has been a major focus of IP theoretical research (e.g., Wynn & King 1995; King & Wynn 1999; Norton et al. 2004). However, authoritative theoretical studies by Norton et al. (2004, 2008) hypothesized that Paloma-like mCVs with large $P_{\text{spin}}/P_{\text{orb}}$ ratios contain secondaries with unusually low magnetic moments and were therefore exceptions to the studies' models of rotational equilibrium.

Norton et al. (2004) predict that synchronization will occur when the magnetic torque exceeds the accretion torque (see also Chanmugam & Ray 1984). So,

$$\frac{\mu_1 \mu_2}{a^3} > \dot{M} \sqrt{GM_1 R_m}, \quad (1)$$

where μ_1 and μ_2 are the respective magnetic moments of the WD and the secondary, a is the binary separation, G is the gravitational constant, M_1 is the WD mass, and R_m is the magnetospheric radius (Norton et al. 2004, their Equation (13)). Within this framework, there are two scenarios under which an mCV could avoid synchronization: a large accretion torque (represented by the right side of Equation (1)) or a low magnetic-locking torque (described by the left side of the equation). The former appears unlikely, based on the weak or absent He II emission in all published spectra of J1344; moreover, the system's absolute magnitude of $G=9.2$ is consistent with low-luminosity IPs (K. Mukai & M. Pretorius 2023, in preparation). This suggests a low mass-transfer rate, which is unsurprising in light of the well-established tendency for mass-transfer rates to be ~ 2 orders of magnitude lower in CVs below the period gap compared to systems above the gap (Knigge et al. 2011).

A lower-than-usual magnetic-locking torque is a more promising explanation, and there are at least two mechanisms that could result in this. First, as Norton et al. (2004, 2008) speculated, the secondary's magnetic moment μ_2 might be very low. The other possibility is that if the WD were unusually massive, its magnetic moment ($\mu_1 = Br^3$) would be lower than for a typical-mass WD of equal surface field strength because of the inverse relation between a WD's mass and its radius. Moreover, increasing the WD's mass would also increase the binary separation a , upon which the magnetic-locking torque has an inverse-cube dependence. Per Equation (1), the opposing accretion torque would also increase with WD mass, albeit with a weaker dependence ($\propto M_1^{1/2}$).

As a quantitative illustration of the massive-WD hypothesis, we consider two hypothetical WD masses ($M_1 = 0.8$ and $1.3 M_\odot$) in a binary with an orbital period of 114 minutes and a secondary mass of $M_2 = 0.1 M_\odot$. Applying the Nauenberg (1972) mass-radius relationship to these two WD masses, the less-massive WD has a radius ~ 2.5 times larger, so its magnetic moment would be higher by a factor of 2.5^3 . The binary separation a would be 14% smaller at $M_1 = 0.8 M_\odot$, and the locking torque ($\propto a^{-3}$) would increase by a factor of 1.56 compared to the higher-mass WD. Together, these two factors would result in a factor of ~ 24 reduction in the locking torque at $M_1 = 1.3 M_\odot$ compared to $M_1 = 0.8 M_\odot$. Moreover, the diminished locking torque for the massive WD would be accompanied by a $\sim 27\%$ increase in the spin-up torque from accretion. Collectively, these considerations suggest that the

mass of the WD can play an important role in determining whether the synchronization requirement in Equation (1) is satisfied.

Given the strong dependence of the locking torque on the WD mass, it will be important for a future study to measure or constrain the WD mass. If the WD turns out to be of typical mass, it would provide indirect support for the Norton et al. (2004, 2008) proposal that the secondary has an unusually low magnetic moment μ_2 .

It is also possible that J1344 is a formerly synchronous polar that is out of equilibrium and in the process of resynchronizing, although we disfavor this possibility for several reasons. First, the most commonly invoked method of desynchronizing a polar is a nova eruption, but there is no evidence of a nova eruption in J1344. The Digital Access to a Sky-Century at Harvard collection of photographic plates (Grindlay et al. 2009) shows no detections at J1344's position, and the spectral energy distribution (Figure 4) is inconsistent with a hot WD. Moreover, the recurrence timescale for novae becomes increasingly long at short orbital periods due to the diminished mass-transfer rates at those periods (e.g., Figure 5 in Knigge et al. 2011), so the likelihood of observing such a system by chance is low. Another difficulty with the nova hypothesis is that the amount of angular momentum required to spin up a previously synchronized WD by a minimum¹⁵ of 10% is immense, particularly when one considers that the prototypical AP, V1500 Cyg, was desynchronized by only 3% following its nova eruption.

Finally, as a corollary to the previous paragraph, it is also conceivable that J1344 is synchronizing for the first time—but here again, we encounter a difficulty with the low probability of observing such a system in a short-lived stage in its overall lifetime. Schreiber et al. (2021) proposed that polars are the descendants of *nonmagnetic* CVs whose WDs began to crystallize after having been spun up by accretion; the emergence of the magnetic field causes the formerly non-magnetic CV to synchronize rapidly. Even the slowest synchronization timescales contemplated by Schreiber et al. (2021) make it improbable that such a system would be serendipitously discovered during this brief process.

5. Conclusion

We have reclassified the nominally synchronous polar SDSS J134441.83+204408.3 as an asynchronous mCV with $P_{\text{spin}}/P_{\text{orb}} = 0.893$, which is simultaneously much more desynchronized than observed in APs but also much more synchronized than seen in IPs. Based on its unusual $P_{\text{spin}}/P_{\text{orb}}$, J1344 bears a striking resemblance to Swift J0503.7-2819 ($P_{\text{spin}}/P_{\text{orb}} = 0.8$) and Paloma ($P_{\text{spin}}/P_{\text{orb}} = 0.87$), but unlike those systems, J1344's magnetic-field strength is easily measurable ($B = 56 \pm 2$ MG). The highly asynchronous nature of J1344 reveals that the combination of $B \gtrsim 10$ MG and a short binary separation does not guarantee that a system will rapidly synchronize. Within the existing theoretical framework, some combination of a weakly magnetic secondary star or an unusually massive WD is the most attractive explanation for the failure of J1344 to achieve synchronous rotation.

¹⁵ If J1344 is in a temporarily desynchronized state due to a long-ago nova eruption, we would expect it to have been even more desynchronized immediately after the nova.

We have tentatively identified the Thorstensen et al. (2020) spectroscopic frequency as the WD spin frequency, but follow-up studies are needed to confirm this. These studies should seek out spectral features that are unambiguously attributable to the secondary (either emission lines from its inner hemisphere or absorption features), although this will be challenging given the late spectral type expected for the secondary at $P_{\text{orb}} = 114$ minutes. Even if it turns out the Thorstensen et al. (2020) frequency is the orbital frequency, our results are not seriously impacted, and the spin-to-orbit ratio would increase only slightly to $P_{\text{spin}}/P_{\text{orb}} = 0.903$.

Finally, J1344's ability to successfully masquerade as a synchronous polar for a decade suggests that other nominally synchronous systems might also be asynchronous. It will be important to examine the TESS light curves of all polars to search for any such systems.

During the preparation of this manuscript, the astronomical community experienced a profound loss with the untimely death of Tom Marsh. Over the course of his career, Tom established himself as both a distinguished researcher and a cherished colleague. His legacy will be felt for many years to come.







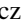


We thank Koji Mukai for helpful comments and for sharing a draft of a forthcoming paper.

Facilities: TESS, Struve, Sloan.

Software: `astropy` (Astropy Collaboration et al. 2018), `lightkurve` (Barentsen et al. 2020).

Note added in proof. After a preprint of this manuscript was made publicly available, Coel Hellier pointed out to us that there is still debate as to whether EX Hya is in rotational equilibrium, for reasons discussed in Hellier (2014). We thank him for pointing this out to us.

ORCID iDs

Colin Littlefield  <https://orcid.org/0000-0001-7746-5795>
 Paul A. Mason  <https://orcid.org/0000-0002-5897-3038>
 Peter Garnavich  <https://orcid.org/0000-0003-4069-2817>
 Paula Szkody  <https://orcid.org/0000-0003-4373-7777>
 John Thorstensen  <https://orcid.org/0000-0002-4964-4144>
 Simone Scaringi  <https://orcid.org/0000-0001-5387-7189>
 Krystian Izkiewicz  <https://orcid.org/0000-0002-4005-5095>
 Mark R. Kennedy  <https://orcid.org/0000-0001-6894-6044>
 Natalie Wells  <https://orcid.org/0000-0003-2101-3540>

References

- Astropy Collaboration, Price-Whelan, A. M., Sipőcz, B. M., et al. 2018, *AJ*, **156**, 123
- Bailer-Jones, C. A. L., Rybizki, J., Fouesneau, M., Demleitner, M., & Andrae, R. 2021, *AJ*, **161**, 147
- Barentsen, G., Hedges, C., Vinícius, Z., et al. 2020, KeplerGO/lightkurve: v2.0b3, Zenodo, doi:[10.5281/zenodo.1181928](https://doi.org/10.5281/zenodo.1181928)
- Channugam, G., & Ray, A. 1984, *ApJ*, **285**, 252
- Channugam, G., & Wagner, R. L. 1979, *ApJ*, **232**, 895
- Cropper, M., Mason, K. O., Allington-Smith, J. R., et al. 1989, *MNRAS*, **236**, 29P
- Ferrario, L., de Martino, D., & Gänsicke, B. T. 2015, *SSRv*, **191**, 111
- Gaia Collaboration, Brown, A. G. A., Vallenari, A., et al. 2021, *A&A*, **649**, A1
- Gaia Collaboration, Prusti, T., de Bruijne, J. H. J., et al. 2016, *A&A*, **595**, A1
- Green, G. M., Schlafly, E., Zucker, C., Speagle, J. S., & Finkbeiner, D. 2019, *ApJ*, **887**, 93
- Grindlay, J., Tang, S., Simcoe, R., et al. 2009, in ASP Conf. Ser. 410, Preserving Astronomy's Photographic Legacy: Current State and the Future of North American Astronomical Plates, ed. W. Osborn & L. Robbins (San Francisco, CA: ASP), 101
- Hakala, P., Ramsay, G., Potter, S. B., et al. 2019, *MNRAS*, **486**, 2549
- Halpern, J. P. 2022, *ApJ*, **934**, 123
- Harrison, T. E., & Campbell, R. K. 2018, *MNRAS*, **474**, 1572
- Hellier, C. 2014, *EPJWC*, **64**, 07001
- Joshi, A., Pandey, J. C., Singh, K. P., & Agrawal, P. C. 2016, *ApJ*, **830**, 56
- King, A. R., & Wynn, G. A. 1999, *MNRAS*, **310**, 203
- Knigge, C., Baraffe, I., & Patterson, J. 2011, *ApJS*, **194**, 28
- Koester, D. 2010, *MmSAI*, **81**, 921
- Littlefield, C., Garnavich, P., Mukai, K., et al. 2019, *ApJ*, **881**, 141
- Littlefield, C., Hoard, D. W., Garnavich, P., et al. 2023, *AJ*, **165**, 43
- Mason, P. A., Liebert, J., & Schmidt, G. D. 1989, *ApJ*, **346**, 941
- Mason, P. A., Littlefield, C., Monroy, L. C., et al. 2022, *ApJ*, **938**, 142
- Mason, P. A., Morales, J. F., Littlefield, C., et al. 2020, *AdSpR*, **66**, 1123
- Nauenberg, M. 1972, *ApJ*, **175**, 417
- Norton, A. J., Butters, O. W., Parker, T. L., & Wynn, G. A. 2008, *ApJ*, **672**, 524
- Norton, A. J., Wynn, G. A., & Somerscales, R. V. 2004, *ApJ*, **614**, 349
- Pirola, V., Vornanen, T., Berdyugin, A., & Coyne, G. V. 2008, *ApJ*, **684**, 558
- Rawat, N., Pandey, J. C., Joshi, A., Scaringi, S., & Yadava, U. 2022, *MNRAS*, **517**, 1667
- Schreiber, M. R., Belloni, D., Gänsicke, B. T., Parsons, S. G., & Zorotovic, M. 2021, *NatAs*, **5**, 648
- Schwarz, R., Schwöpe, A. D., Staude, A., et al. 2007, *A&A*, **473**, 511
- Schwöpe, A. D., Buckley, D. A. H., O'Donoghue, D., et al. 1997, *A&A*, **326**, 195
- Szkody, P., Anderson, S. F., Brooks, K., et al. 2011, *AJ*, **142**, 181
- Szkody, P., Everett, M. E., Howell, S. B., et al. 2014, *AJ*, **148**, 63
- Thorstensen, J. R., Motsoaledi, M., Woudt, P. A., Buckley, D. A. H., & Warner, B. 2020, *AJ*, **160**, 70
- Tovmassian, G., González-Buitrago, D., Thorstensen, J., et al. 2017, *A&A*, **608**, A36
- Vaeth, H. 1997, *A&A*, **317**, 476
- Wang, Q., Qian, S., & Liao, W. 2021, *PASP*, **133**, 114201
- Wynn, G. A., & King, A. R. 1995, *MNRAS*, **275**, 9